

---

# Gaussian Process Regression in Logarithmic Time

---

Adrien Corenflos<sup>1</sup>

Zheng Zhao<sup>1</sup>

Simo Särkkä<sup>1</sup>

<sup>1</sup>Department of Electrical Engineering and Automation, Aalto University, Finland

## Abstract

The aim of this article is to present a novel parallelization method for temporal Gaussian process (GP) regression problems. The method allows for solving GP regression problems in logarithmic  $O(\log N)$  time, where  $N$  is the number of time steps. Our approach uses the state-space representation of GPs which in its original form allows for linear  $O(N)$  time GP regression by leveraging the Kalman filtering and smoothing methods. By using a recently proposed parallelization method for Bayesian filters and smoothers, we are able to reduce the linear computational complexity of the Kalman filter and smoother solutions to the GP regression problems into logarithmic span complexity, which transforms into logarithm time complexity when implemented in parallel hardware such as a graphics processing unit (GPU). We experimentally demonstrate the computational benefits on one simulated and real datasets via our open-source implementation leveraging the GPflow framework.

## 1 INTRODUCTION

Gaussian processes (GPs) [Rasmussen and Williams, 2006] are a family of useful priors used to solve regression and classification problems arising in machine learning. In their naive form their complexity scales as  $O(N^3)$  where  $N$  is the number of training data points, which is problematic with large datasets. In literature people have proposed using sparse GP methods, based on introducing  $U \ll N$  inducing points, spectral samples, or basis functions which can reduce the complexity down to  $O(U^2 N)$  [Rasmussen and Williams, 2006, Quiñero-Candela and Rasmussen, 2005, Lázaro-Gredilla et al., 2010, Hensman et al., 2017, Solin and Särkkä, 2020]. However, the positions/shapes and numbers of inducing points or basis functions must typically be

determined by either human experts or learned from data. Additionally for certain datasets and covariance functions choices, finding such sparse representation might prove difficult.

In the case of temporal or spatio-temporal GPs we can use state-space smoothing methods [Hartikainen and Särkkä, 2010, Särkkä et al., 2013] which scale linearly ( $O(N)$ ) in the number of training and test points. The idea is to reformulate the GPs as solutions to stochastic differential equations (SDEs). By using this representation one can then leverage the Markov property and reduce the regression computational complexity from cubic to linear via the Kalman filter and RTS smoother methods [Hartikainen and Särkkä, 2010].

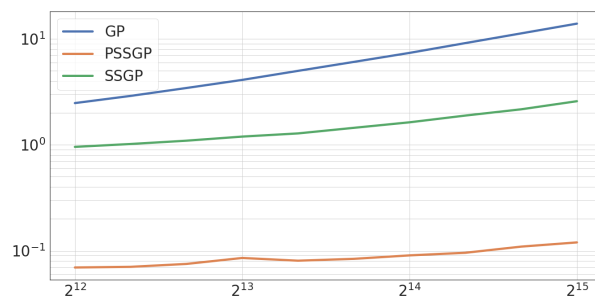


Figure 1: Average run time in seconds of predicting  $M = 10000$  test points for noisy sinusoidal data with RBF covariance function for standard GP, SSGP, and PSSGP (ours). x-axis is the number of training data points  $N$ . We can see that our method outperforms GP and SSGP by a factor 10.

The aim of this article is to develop parallel state-space GPs (PSSGPs) methods with which the computational complexity (in the sense of parallel span complexity) reduces to logarithmic  $O(\log N)$  in the number of data points, both at training and inference time (see Fig. 1). The conventional Kalman filter and smoother based state-space GPs (SSGPs) are not easily parallelizable as such and require  $O(N)$  time also when run in parallel architectures. However,

Särkkä and Ángel F. García-Fernández [2021] showed that by converting the Kalman filter and smoother into an associative operator form it is possible to reduce their time (i.e., span) complexity to  $O(\log N)$ . This proves highly beneficial on parallel architectures such as graphic processing units (GPU) or the more recent tensor processing units (TPU) [Jouppi et al., 2017]. In particular, one may then resort to modern computational libraries such as TensorFlow to optimize the hyperparameters of the GP model via automatic differentiation at a  $O(\log N)$  cost.

As shown in [Grigorievskiy et al., 2017], is also possible to leverage the sparse matrix structure induced by state-space representation together with parallel matrix computations to induce parallelism. This approach is related to the stochastic partial differential equation (SPDE) methods for Gaussian Markov fields [Lindgren et al., 2011] where parallel matrix computations also provide computational benefits. However, although these methods can also reach  $O(\log N)$  span complexity in some special cases, they require computations with large (although sparse) matrices – which can be memory expensive – and the logarithmic span complexity is hard to guarantee for all the subproblems [Grigorievskiy et al., 2017]. Other approaches to parallelization of Gaussian processes include, for example, local approximations and mixtures of experts [Low et al., 2015, Liu et al., 2018, Zhang and Williamson, 2019].

The contribution of our paper is four-fold:

1. We combine the formulation of state-space GPs with parallel representation of Kalman filters.
2. We extend the parallel formulation to missing measurements for prediction in state-space GPs.
3. We implement parallelized parameter learning via likelihood maximization and Hamiltonian Monte Carlo methods on GPU.
4. The method has been implemented as an extensible library leveraging the GPflow framework, which can be accessed at <https://github.com/EEA-sensors/parallel-gps>.

In Section 2, we review the main results on the state-space representation of Gaussian processes. In Section 3 we extend the formulation of parallel Kalman filtering and smoothing to the case when there exist missing observations, which is necessary for its use in Gaussian processes regression problems. In Section 4 we then describe the end-to-end parallel formulation of state space Gaussian processes. Finally in Section 5 we illustrate the benefits and limitations of our approach for prediction and parameters learning on a toy-model and two real datasets.

## 2 STATE-SPACE GAUSSIAN PROCESSES

In this section, we quickly recall results about the state-space formulation of Gaussian processes and present their temporal parallelization formulation.

### 2.1 GPS IN STATE-SPACE FORM

As shown in Hartikainen and Särkkä [2010], a temporal GP regression problem of the form

$$\begin{aligned} f(t) &\sim \text{GP}(0, C(t, t')), \\ y_k &= f(t_k) + e_k, \quad e_k \sim \mathcal{N}(0, \sigma_k^2), \end{aligned} \quad (1)$$

where  $k = 1, \dots, N$ , can be converted into a smoothing problem for a  $n_x$ -dimensional continuous-discrete state-space model,

$$\begin{aligned} \frac{d\mathbf{x}(t)}{dt} &= \mathbf{G}\mathbf{x}(t) + \mathbf{L}\mathbf{w}(t), \\ y_k &= \mathbf{H}\mathbf{x}(t_k) + e_k, \end{aligned} \quad (2)$$

where  $n_x$  depends on the covariance function at hand,  $f(t) \triangleq \mathbf{H}\mathbf{x}(t)$ , and with initial conditions taken to be at its steady-state

$$\mathbf{x}(t_0) \sim \mathcal{N}(\mathbf{0}, \mathbf{P}_\infty), \quad (3)$$

where  $\mathbf{P}_\infty$  is the solution of the Lyapunov equation [Brogan, 2011]

$$\mathbf{0} = \mathbf{G}^\top \mathbf{P}_\infty + \mathbf{P}_\infty \mathbf{G} + \mathbf{L}\mathbf{Q}\mathbf{L}^\top. \quad (4)$$

This is especially true in the case of Matérn kernels where this representation is exact and available in closed form [Hartikainen and Särkkä, 2010], while more general stationary covariance functions such as the radial basis function (RBF) can be approximated by a system of the form (2) of increasing dimension up to an arbitrary precision by using Taylor series or Páde approximants [Hartikainen and Särkkä, 2010, Särkkä and Piché, 2014] in spectral domain. State-space representations of various other covariance functions have been reviewed in Solin [2016] and Särkkä and Solin [2019].

For instance, the state-space formulation for Matérn 3/2 covariance function is

$$\begin{aligned} C_{\text{Mat.}}(t, t') &= \sigma^2 \left( 1 + \frac{\sqrt{3}|t-t'|}{\ell} \right) \\ &\quad \times \exp\left(-\frac{\sqrt{3}|t-t'|}{\ell}\right), \end{aligned} \quad (5)$$

has the state-space representation

$$\mathbf{G} = \begin{pmatrix} 0 & 1 \\ -\lambda^2 & -2\lambda \end{pmatrix}, \quad \mathbf{L} = \begin{pmatrix} 0 \\ 1 \end{pmatrix}, \quad \mathbf{P}_0 = \begin{pmatrix} \sigma^2 & 0 \\ 0 & \lambda^2 \sigma^2 \end{pmatrix}, \quad (6)$$

where  $\lambda = \sqrt{3}/\ell$ . The spectral density of the corresponding white noise is  $q = 4\lambda^3 \sigma^2$ . The measurement model matrix is  $\mathbf{H} = (1 \ 0)$ .

## 2.2 GP INFERENCE AS KALMAN FILTERING AND SMOOTHING

The continuous-time state-space model (2) can be discretized into a discrete-time linear Gaussian state space model (LGSSM, e.g., [Särkkä and Solin, 2019]) of the form

$$\begin{aligned}\mathbf{x}_k &= \mathbf{F}_{k-1} \mathbf{x}_{k-1} + \mathbf{q}_{k-1} \\ y_k &= \mathbf{H} \mathbf{x}_k + e_k,\end{aligned}\quad (7)$$

where  $\mathbf{q}_{k-1} \sim \mathcal{N}(\mathbf{0}, \mathbf{Q}_{k-1})$  and  $e_k \sim N(0, \sigma_k)$ .

In the above model,

$$\begin{aligned}\mathbf{F}_{k-1} &= \exp((t_k - t_{k-1}) \mathbf{G}), \\ \mathbf{Q}_{k-1} &= \int_0^{t_k - t_{k-1}} \exp((t_k - t_{k-1} - s) \mathbf{G}) \\ &\quad \times \mathbf{L} \mathbf{q} \mathbf{L}^\top \exp((t_k - t_{k-1} - s) \mathbf{G})^\top ds.\end{aligned}\quad (8)$$

The GP regression problem can now be solved by applying Kalman filter and smoother algorithms on the model (7) [Hartikainen and Särkkä, 2010].

## 2.3 PARAMETER LEARNING IN STATE-SPACE GPS

Additionally  $C(t, t')$  and  $\sigma_k^2$  in Equation (1) may depend on hyperparameters  $\boldsymbol{\theta} : C(t, t'; \boldsymbol{\theta}), \sigma_k^2(\boldsymbol{\theta})$  that need to be learned. To this end one can rely on likelihood-based techniques that require to compute the marginal likelihood of the observations  $p(y_1, \dots, y_N | \boldsymbol{\theta})$ , which can be done, given the filtering density  $p(\mathbf{x}_k | y_1, \dots, y_k, \boldsymbol{\theta}) = \mathcal{N}(\mathbf{x}_k | \boldsymbol{\mu}_k(\boldsymbol{\theta}), \mathbf{P}_k(\boldsymbol{\theta}))$ , through the identity

$$p(y_1, \dots, y_N | \boldsymbol{\theta}) = \prod_{k=1}^N \mathcal{N}(y_k | \boldsymbol{\mu}_k(\boldsymbol{\theta}), V_k(\boldsymbol{\theta})), \quad (9)$$

where  $\boldsymbol{\mu}_k = \mathbf{H} \mathbf{F}_{k-1} \mathbf{m}_{k-1}$  is the predictive observation mean and  $V_k = \mathbf{H} [\mathbf{F}_{k-1} \mathbf{P}_{k-1} \mathbf{F}_{k-1}^\top + \mathbf{Q}_{k-1}] \mathbf{H}^\top + \sigma_k^2$  is the observation predictive variance, and we have omitted the dependency on  $\boldsymbol{\theta}$  for notational simplicity.

For example, we may then compute the maximum likelihood estimate (MLE) by maximizing Equation (9) or equivalently its logarithm, or more generally, we can also compute the maximum a posteriori of the parameters  $\boldsymbol{\theta}$  if they are considered to have a prior distribution  $p(\boldsymbol{\theta})$  by maximizing instead  $p(\boldsymbol{\theta} | y_1, \dots, y_N) \propto p(y_1, \dots, y_N | \boldsymbol{\theta}) p(\boldsymbol{\theta})$ . Finally, we can also sample from the posterior distribution  $p(\boldsymbol{\theta} | y_1, \dots, y_N)$  using Markov chain Monte Carlo, and in particular if we have access to its gradient with respect to  $\boldsymbol{\theta}$ , via Hamiltonian Monte Carlo [Neal, 2011]. Computing these gradients has been made easier through the advent of automatic differentiation libraries such as TensorFlow [Abadi et al., 2015], which we exploit in the experiments of this paper (in Section 5) by extending GPflow [Matthews et al., 2017].

## 3 TEMPORAL PARALLELIZATION OF KALMAN EQUATIONS

The formulation in terms of a continuous state space model presented in the previous section reduced the computational complexity of inference in compatible GPs to  $O(N)$  instead of the cubic cost induced by naive GP methods or to a lesser extent by their sparse approximations [Rasmussen and Williams, 2006]. In this section, we show how by using and extending the parallel state-space methodology of Särkkä and Ángel F. García-Fernández [2021] we can reduce the parallel computational complexity (i.e., the span complexity) down to  $O(\log N)$ .

### 3.1 PARALLEL KALMAN FILTER

In Särkkä and Ángel F. García-Fernández [2021], the authors introduce an equivalent formulation of Kalman filters and smoothers in terms of an associative operator that enables them to leverage distributed implementations of scan (prefix-sum) algorithms such as Blelloch [1989, 1990]. However their formulation doesn't consider the possibility of missing observations, which is a critical characteristic of inference in state space GP models to do a prediction on the test points [Särkkä et al., 2013], we therefore extend their derivation to take these into account.

The method in Särkkä and Ángel F. García-Fernández [2021] consists in representing the filter in terms of five quantities  $\mathbf{A}, \mathbf{b}, \mathbf{C}, \boldsymbol{\eta}, \mathbf{J}$ , which are first initialized in parallel and then combined using parallel associative scan [Blelloch, 1989, 1990]. In order to cope with the missing observations, the initialization needs to be modified. At the time steps  $k$ , where we have an observation, we initialize in the same way as in the original method:

$$\begin{aligned}\mathbf{A}_k &= (\mathbf{I}_{n_x} - \mathbf{K}_k \mathbf{H}) \mathbf{F}_{k-1}, \\ \mathbf{b}_k &= \mathbf{K}_k \mathbf{y}_k, \\ \mathbf{C}_k &= (\mathbf{I}_{n_x} - \mathbf{K}_k \mathbf{H}) \mathbf{Q}_{k-1}, \\ \mathbf{K}_k &= \mathbf{Q}_{k-1} \mathbf{H}^\top \mathbf{S}_k^{-1}, \\ \mathbf{S}_k &= \mathbf{H} \mathbf{Q}_{k-1} \mathbf{H}^\top + \mathbf{R}_k,\end{aligned}\quad (10)$$

and for  $k = 1$  as

$$\begin{aligned}\mathbf{S}_1 &= \mathbf{H} \mathbf{P}_\infty \mathbf{H}^\top + \mathbf{R}_1, \\ \mathbf{K}_1 &= \mathbf{P}_\infty \mathbf{H}^\top \mathbf{S}_1^{-1}, \\ \mathbf{A}_1 &= \mathbf{0}, \\ \mathbf{b}_1 &= \mathbf{K}_1 \mathbf{y}_1, \\ \mathbf{C}_1 &= \mathbf{P}_\infty - \mathbf{K}_1 \mathbf{S}_1 \mathbf{K}_1^\top.\end{aligned}\quad (11)$$

The parameters of the second term are given as

$$\begin{aligned}\boldsymbol{\eta}_k &= \mathbf{F}_{k-1}^\top \mathbf{H}^\top \mathbf{S}_k^{-1} \mathbf{y}_k, \\ \mathbf{J}_k &= \mathbf{F}_{k-1}^\top \mathbf{H}^\top \mathbf{S}_k^{-1} \mathbf{H} \mathbf{F}_{k-1},\end{aligned}\quad (12)$$

for  $k = 1, \dots, N$ . In our case we actually have scalar observations and  $\mathbf{R}_k = \sigma_k$ , but we have retained the possibility for processing multiple observations at a time step by letting the  $\mathbf{y}_k$  to be a vector and  $\mathbf{R}_k$  a matrix. In the remainder of this article we only consider uni-dimensional observations  $y_k$ 's but the equations above could also be used for multi-dimensional ones where the observation matrices would only need to be stacked together.

In the case when  $k$  corresponds to a missing observation we initialize in a slightly different way. By noticing that  $f_k(\mathbf{x}_k | \mathbf{x}_{k-1})$  reduces to the transition distribution  $p(\mathbf{x}_k | \mathbf{x}_{k-1}) = \mathcal{N}(\mathbf{x}_k | \mathbf{F}_{k-1}\mathbf{x}_{k-1}, \mathbf{Q}_{k-1})$  for  $k > 1$  and  $p(\mathbf{x}_1)$  for  $k = 1$  so that initialization Equations (10), (11) and (12) in the steady-state of the reduce to the following equations

$$\begin{aligned} \mathbf{A}_k &= \mathbf{F}_{k-1}, \\ \mathbf{b}_k &= \mathbf{0}, \\ \mathbf{C}_k &= \mathbf{Q}_{k-1} \end{aligned} \quad (13)$$

for  $k > 1$ , and for  $k = 1$  as

$$\begin{aligned} \mathbf{A}_1 &= \mathbf{0}, \\ \mathbf{b}_1 &= \mathbf{0}, \\ \mathbf{C}_1 &= \mathbf{P}_\infty, \end{aligned} \quad (14)$$

with for all  $k$ ,

$$\begin{aligned} \boldsymbol{\eta}_k &= \mathbf{0}, \\ \mathbf{J}_k &= \mathbf{0}. \end{aligned} \quad (15)$$

We prove that these equations indeed recover the filtering distribution in the Supplementary.

When the quantities  $\mathbf{A}, \mathbf{b}, \mathbf{C}, \boldsymbol{\eta}, \mathbf{J}$  have been initialized they can then be combined using parallel scan, with the associative operator

$$\begin{aligned} &(\mathbf{A}_{ij}, \mathbf{b}_{ij}, \mathbf{C}_{ij}, \boldsymbol{\eta}_{ij}, \mathbf{J}_{ij}) \\ &= (\mathbf{A}_i, \mathbf{b}_i, \mathbf{C}_i, \boldsymbol{\eta}_i, \mathbf{J}_i) \otimes (\mathbf{A}_j, \mathbf{b}_j, \mathbf{C}_j, \boldsymbol{\eta}_j, \mathbf{J}_j) \end{aligned}$$

defined in the same way as in Särkkä and Ángel F. García-Fernández [2021]:

$$\begin{aligned} \mathbf{A}_{ij} &= \mathbf{A}_j (\mathbf{I}_{n_x} + \mathbf{C}_i \mathbf{J}_j)^{-1} \mathbf{A}_i, \\ \mathbf{b}_{ij} &= \mathbf{A}_j (\mathbf{I}_{n_x} + \mathbf{C}_i \mathbf{J}_j)^{-1} (\mathbf{b}_i + \mathbf{C}_i \boldsymbol{\eta}_j) + \mathbf{b}_j, \\ \mathbf{C}_{ij} &= \mathbf{A}_j (\mathbf{I}_{n_x} + \mathbf{C}_i \mathbf{J}_j)^{-1} \mathbf{C}_i \mathbf{A}_j^\top + \mathbf{C}_j, \\ \boldsymbol{\eta}_{ij} &= \mathbf{A}_i^\top (\mathbf{I}_{n_x} + \mathbf{J}_j \mathbf{C}_i)^{-1} (\boldsymbol{\eta}_j - \mathbf{J}_j \mathbf{b}_i) + \boldsymbol{\eta}_i, \\ \mathbf{J}_{ij} &= \mathbf{A}_i^\top (\mathbf{I}_{n_x} + \mathbf{J}_j \mathbf{C}_i)^{-1} \mathbf{J}_j \mathbf{A}_i + \mathbf{J}_i. \end{aligned}$$

Running a prefix-sum algorithm on the elements above with the filtering operator  $\otimes$  then produces a sequence of elements  $(\mathbf{A}_k^*, \mathbf{b}_k^*, \mathbf{C}_k^*, \boldsymbol{\eta}_k^*, \mathbf{J}_k^*)$ ,  $k = 1, \dots, N$ , of which the terms  $\bar{\mathbf{x}}_k \triangleq \mathbf{b}_k^*$  and  $\mathbf{P}_k \triangleq \mathbf{C}_k^*$  will then correspond to the filtering mean and covariance at time  $k$ , respectively.

**Proposition 1** (Equivalence of sequential and parallel Kalman filters). *For all  $k = 1, 2, \dots, N+M$  the Kalman filter means and covariances are given by  $\bar{\mathbf{x}}_k = \mathbf{b}_k^*$  and  $\mathbf{P}_k = \mathbf{C}_k^*$ , respectively.*

This proof of this proposition is a bit lengthy and therefore can be found in the Supplementary material.

**Remark 1.** *The initialization Equations (13), (14), and (15) in the case of missing observations can intuitively be understood as taking the local as taking the local gain  $\mathbf{K}_k$  approaching zero in Equations (10), (11), and (12), respectively, or more generally as taking the limit of measurement noise variance  $\mathbf{R}$  to approach infinity.*

### 3.2 PARALLEL RAUCH-TUNG-STRIEBEL SMOOTHER

The prediction step of the GP then corresponds to running a Kalman smoother (Rauch–Tung–Striebel smoother, see Hartikainen and Särkkä [2010], Särkkä et al. [2013]) on the filtering means and covariances  $\bar{\mathbf{x}}_k$  and  $\mathbf{P}_k$  obtained in parallel in the previous section. We show in the Supplementary that this can be done in parallel using the method proposed in Särkkä and Ángel F. García-Fernández [2021] even when some observations are missing.

Similarly to parallel filter we first need to initialize the elements that will be passed to the associative scan algorithm. This can be done in parallel in the following way.

For  $k < N$  we have:

$$\begin{aligned} \mathbf{E}_k &= \mathbf{P}_k \mathbf{F}_k^\top \left( \mathbf{F}_k \mathbf{P}_k \mathbf{F}_k^\top + \mathbf{Q}_k \right)^{-1}, \\ \mathbf{g}_k &= \bar{\mathbf{x}}_k - \mathbf{E}_k (\mathbf{F}_k \bar{\mathbf{x}}_k), \\ \mathbf{L}_k &= \mathbf{P}_k - \mathbf{E}_k \mathbf{F}_k \mathbf{P}_k, \end{aligned}$$

and for  $k = N$  we have

$$\begin{aligned} \mathbf{E}_N &= \mathbf{0}, \\ \mathbf{g}_N &= \bar{\mathbf{x}}_N, \\ \mathbf{L}_N &= \mathbf{P}_N. \end{aligned}$$

We can then define the associative operator

$$(\mathbf{E}_{ij}, \mathbf{g}_{ij}, \mathbf{L}_{ij}) = (\mathbf{E}_i, \mathbf{g}_i, \mathbf{L}_i) \otimes (\mathbf{E}_j, \mathbf{g}_j, \mathbf{L}_j)$$

corresponding to the smoothing operation is then defined as

$$\begin{aligned} \mathbf{E}_{ij} &= \mathbf{E}_i \mathbf{E}_j, \\ \mathbf{g}_{ij} &= \mathbf{E}_i \mathbf{g}_j + \mathbf{g}_i, \\ \mathbf{L}_{ij} &= \mathbf{E}_i \mathbf{L}_j \mathbf{E}_i^\top + \mathbf{L}_i. \end{aligned}$$

Similarly to the filtering case, running a now backward prefix sum algorithm produces the elements  $(\mathbf{E}_k^s, \mathbf{g}_k^s, \mathbf{L}_k^s)$  for  $k = 1, \dots, N$  such that the smoothing means and covariances can be recovered as  $\mathbf{m}_k^s = \mathbf{g}_k^s$  and  $\mathbf{P}_k^s = \mathbf{L}_k^s$ , respectively.

**Proposition 2** (Equivalence of sequential and parallel Kalman smoothers). *For all  $k = 1, 2, \dots, N + M$  the Kalman smoother means and covariances are given by  $\mathbf{m}_k^s = \mathbf{g}_k^*$  and  $\mathbf{P}_k^s = \mathbf{L}_k^*$  respectively.*

The proof of the above proposition can be found in the Supplementary material.

## 4 TEMPORAL PARALLELIZATION OF GAUSSIAN PROCESSES

A direct consequence of Propositions 1 and 2 is the fact that the parallel and sequential versions of SSGP are equivalent, so that their solutions will recover the same distribution.

In this section, we now provide the details of the steps needed to create the linear Gaussian state-space model (LGSSM) representation of state-space GPs so that the end-to-end algorithm is parallelizable across the time dimension, resulting a total span complexity of  $O(\log N)$  in the number of observations  $N$ , from training to inference.

### 4.1 COMPUTATION OF THE STEADY-STATE COVARIANCE

To represent a stationary GP one must start the state-space model SDE from the stationary initial condition Hartikainen and Särkkä [2010]. The (steady-state) initial covariance can be computed by solving the Lyapunov equation (4). The complexity of this step is independent of the number of time steps and does not need explicit time-parallelization.

There exists a number of iterative methods for solving this kind of algebraic equations [Hodel et al., 1996]. However, in order to make automatic differentiation efficient, in this work, we used the closed form vectorization solution given in Brogan [2011] (p. 229) which relies on matrix algebra, and does not need any explicit looping. This is feasible because we only need to numerically solve the Lyapunov equation for small state dimensions. Furthermore, as this solution only involves matrix inversions and multiplications, it is easily parallelizable on GPU architectures.

### 4.2 BALANCING OF THE STATE SPACE MODEL

In practice the state space model obtained via discretization in Section 2 might be numerically unstable due to the transition matrix having a poor conditioning number, this would in turn result in inaccuracies in computing both the GP predictions and the marginal log-likelihood of the observations. To mitigate this issue we resort to balancing [Osborne, 1960] in order to obtain a transition matrix  $\mathbf{F}$  which has rows and columns that have equal norms, therefore obtaining a more stable auxiliary state space model. For any diagonal matrix

$\mathbf{D} \in \mathbb{R}^{n_x \times n_x}$ , the continuous-discrete model

$$\begin{aligned} \frac{d\mathbf{z}(t)}{dt} &= \mathbf{D}^{-1} \mathbf{G} \mathbf{D} \mathbf{z}(t) + \mathbf{D}^{-1} \mathbf{L} \mathbf{w}(t), \\ y_k &= \mathbf{H} \mathbf{D} \mathbf{z}_k + e_k, \end{aligned} \quad (16)$$

with initial condition given by  $\mathbf{z}(0) \sim \mathcal{N}(\mathbf{0}, \mathbf{D}^{-1} \mathbf{P}_\infty \mathbf{D})$  is an equivalent representation of the state-space model (2) with initial covariance given by  $\mathbf{x}(0) \sim \mathcal{N}(\mathbf{0}, \mathbf{P}_\infty)$  with  $\mathbf{P}_\infty$  given in Equation (3), in the sense that for all  $t$ ,

$$f(t) = \mathbf{H} \mathbf{D} \mathbf{z}(t).$$

In particular it means that the gradient of  $p(y_1, \dots, y_N | \boldsymbol{\theta})$  with respect to the covariance function and observation model parameters  $\boldsymbol{\theta}$  is left unchanged by the choice of scaling matrix  $\mathbf{D}$ . This property allows us to condition our state space representation of the original GP using the scaling matrix  $\mathbf{D}^*$  defined in Osborne [1960], and to compute the gradient of the marginal log-likelihood of the observations with respect to the GP hyperparameters as if  $\mathbf{D}^*$  did not depend on  $\mathbf{F}$  and therefore the hyperparameters  $\boldsymbol{\theta}$ . This is critical to obtain a stable gradient while not having to unroll the loop necessary to compute  $\mathbf{D}^*$ .

### 4.3 CONVERTING GPS INTO DISCRETE-TIME STATE SPACE

In order to use the parallel formulation of Kalman filters and smoothers in Section 3 we need to first form the continuous state space model representation from the initial Gaussian process definition. This operation is independent of the number of measurements and therefore has a complexity of  $O(1)$ . When it has been formed, we then need to transform it into a discrete-time LGSSM via the equations (8). In practice, the discretization can be implemented using, for example, matrix fractions or various other methods [Axelsson and Gustafsson, 2014, Särkkä and Solin, 2019]. These operations are fully parallelizable across the time dimension and therefore have a span complexity of  $O(1)$  when run on a parallel architecture.

It is worth noting that at learning phase, the discretization only needs to happen at the training data points, therefore not involving any further data manipulation. However, when predicting, it is necessary to insert the  $M$  requested prediction times at the right location in the training data set in order to be able to run the Kalman filter and smoother routines. When done naively, this operation has a complexity  $O(M + N)$  using merging operation [Cormen et al., 2009], however it can be done in parallel with a span complexity of  $O(\log(\min(M, N)))$ . In addition, for some GP models, such as Matérn GPs the discretization can be done offline, because the discretization admits closed-forms.

#### 4.4 END-TO-END COMPLEXITY ANALYSIS OF PARALLELIZED STATE SPACE GPs

The complexity analysis of the six stages for running the parallelized state space GPs are in the following.

1. Complexity of forming the continuous state-space model is  $O(1)$  in both work and span complexities.
2. Complexity of discretizing the state-space model is  $O(N)$  is work complexity and  $O(1)$  in span complexity.
3. Complexity of the parallel Kalman filtering and smoothing operations for training is of  $O(N)$  in work complexity and  $O(\log N)$  is span complexity.
4. Complexity of merging the data for the prediction is of work complexity  $O(N + M)$  and of span complexity  $O(\log(\min(M, N)))$ .
5. Complexity of the parallel Kalman filtering and smoothing operations for prediction is of  $O(N + M)$  in work complexity and  $O(\log(N + M))$  is span complexity.
6. Automatic differentiation as an adjoint operation has the same computational graph as the parallel Kalman filters and smoothers, and therefore has the same complexities as the training step,  $O(N)$  and  $O(\log N)$ .

Putting together the above we can conclude that the total work and span complexities of doing end-to-end inference to prediction on parallelized state space GPs are  $O(N + M)$  and  $O(\log(N + M))$ , respectively.

## 5 EXPERIMENTS

In this section, we illustrate the benefits of our approach for inference and prediction on simulated and real datasets. Because GPUs are inherently massively parallelized architectures, they are typically not optimized for sequential data processing, exposing a lower clock speed than cost-comparable CPUs. This makes running the standard state space GPs on GPU less attractive than running them on CPU, contrarily to standard GPs which can leverage parallelized linear algebra routines offered by modern GPU architectures. In order to offer a fair comparison between our proposed methodology, the standard GPs implementation, and the standard state space GPs, we have therefore chosen to run the sequential implementation of state space GP on CPU while we run the standard GP and our proposed parallel state space GP on GPU. We verified empirically that running the standard state space GP on the same GPU architecture resulted in a tremendous performance loss for it ( $\sim 100x$  slower), this justifies running it on CPU for benchmarking. All the results were obtained on using an AMD<sup>®</sup> Ryzen threadripper 3960x CPU with 128 GB DDR4 RAM, and an Nvidia<sup>®</sup> GeForce RTX 3090 GPU with 24GB memory.

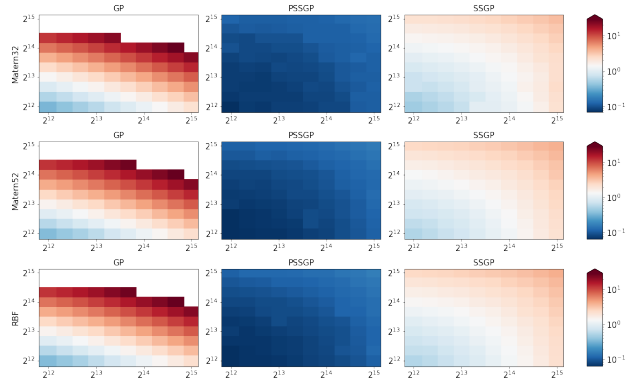


Figure 2: Heatmap of wall time for predicting with GP, SSGP, and PSSGP. y-axis is the number of training data points, x-axis the number of test data points.

### 5.1 TOY MODEL

We first study the behavior of our proposed methodology on a simple sinusoidal model given by

$$f(t) = \sin(\pi t) + \sin(2\pi t) + \sin(3\pi t) \quad (17)$$

$$y_k = f(t_k) + r_k,$$

with observations and prediction times being equally spaced on  $(0, 4)$ , by increasing the number of training or testing points we can therefore demonstrate the empirical time complexity (in terms of wall clock or work span) of our proposed method compared to the standard GP and state space GP.

**Prediction** We first present the results of running a prediction on test points given some input data for a standard GP, state space GP, and our proposed parallel state space GP on the sinusoidal data. We have taken the kernels to be successively Matérn32, Matérn52, and RBF (approximated to the 6th order for the state space GPs), corresponding to  $n_x = 2, 3, 6$  respectively. The training dataset and test dataset have sizes ranging from  $2^{12}$  to  $2^{15}$ . As can be seen in Figures 1 and 2, our proposed method consistently outperforms standard GP and SSGP across the chosen range of dataset sizes with standard GP eventually running out of memory for too big datasets.

**Hyperparameters learning** This speed improvement, while interesting for simple prediction becomes critical when one needs to learn the model hyperparameters, for instance via maximum a posteriori (MAP) or in a fully Bayesian fashion using Markov chain Monte Carlo methods such as Hamiltonian Monte Carlo. Indeed, in this instance, not only does the user need to compute the marginal log-likelihood of the observations, they also need to compute its gradient with respect to the parameters at hand in a timely manner so as to be able to sample from (or to find the maximum of) the posterior distribution of the GP parameters efficiently. While for small enough datasets it is efficiently achieved on GPU using automatic differentiation

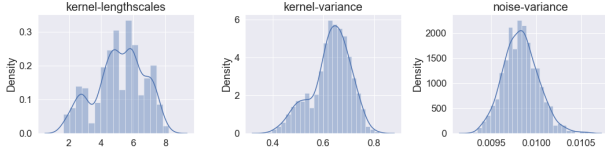


Figure 3: Posterior distribution of the GP parameters for PSSGP. From left to right: kernel lengthscale, kernel variance, and observation model variance.

provided by frameworks such as GPflow Matthews et al. [2017] (relying on Abadi et al. [2015] to eventually compute the reverse mode gradients), this is not the case for longer datasets which arise in real-life. In this section we illustrate the benefits of our proposed algorithm to sample from the posterior distribution of the lengthscale, variance and observation noise of a GP process with Matérn32 kernel using the same data as generate above. The lengthscale, variance and observation noise were chosen to have priors given by Normal distributions of means and variances (1, 3), (1, 3), and (0.1, 1) respectively. To do this we are sampling 1000 times from our posterior distribution using 10 parallel HMC chains Neal [2011] with step-size  $1e-2$ , 10 leapfrog steps, and 100 burn-in samples. In Figure 3 we show the posterior samples obtained in  $\sim 10$  minutes using PSSGP on the sine model with 5500 training points (i.e.  $<1s$  per gradient/log-likelihood evaluation); the standard GP took 8 hours to run (but necessitated using double float precision while state space GPs ran using single float precision) while the SSGP took about 13 hours.

## 5.2 SUNSPOTS DATASET

In this section we compare regression and parameter learning on the monthly sunspot activity dataset by World Data Center SILSO, Royal Observatory of Belgium, Brussels<sup>1</sup>. The number of total training points in this dataset is  $N = 3,200$  for learning the GP hyperparameters. We interpolate the data for every single day from 1749-01-31 to 2018-07-31 which results in 96,000 prediction points.

Table 1: Running time of hyperparameter learning on sunspot dataset relative to PSSGP. The PSSGP took 39, 46, and 48 milliseconds per function/gradient evaluation when  $N = 1200, 2200$ , and  $3200$ , respectively.

N	GP	SSGP	PSSGP
1200	1.03	12.08	<b>1</b>
2200	3.82	25.7	<b>1</b>
3200	10.1	43.86	<b>1</b>

The results of running time is shown in the above Table 1. PSSGP is shown to be the fastest for all  $N$ . Moreover,

<sup>1</sup>The data is available at <http://www.sidc.be/silso/datafiles>

PSSGP is  $\times 10$  and  $43x$  faster than GP and SSGP when  $N = 3200$ . Interpolating daily then took 0.14s for PSSGP, while SSGP on CPU and GP on GPU where respectively 23 and 33 times slower.

## 5.3 CO2 CONCENTRATION DATASET

In order to understand the impact of dimensionality of the SDE we finally consider the Mauna Loa carbon dioxide concentration dataset<sup>2</sup>. We selected monthly and weekly data from year 1974 to 2021 which contains 3192 training points. To model the periodic pattern of the data, we use the following composite covariance function

$$C_{\text{co2}}(t-t') = C_{\text{Per.}}(t-t')C_{\text{Mat.}}(t-t') + C_{\text{Mat.}}(t-t'). \quad (18)$$

This is slightly different from the one suggested in [Solin and Särkkä, 2014] where the authors also add a RBF covariance to  $C_{\text{co2}}$ , however we did not see any improvement in RMSE from adding this supplementary degree of freedom and therefore removed it so as to make the system more easily identifiable. This covariance function cannot be represented exactly by a finite dimensional SDE due to the presence of the quasi-periodic covariance function. However it can be approximated using Taylor expansion methods up to an arbitrary order Solin and Särkkä [2014] resulting in a state of increasing dimension: first, second, and third order will result in an SDE of dimension  $n_x = 10, 14$ , and 18 respectively.

Table 2: Relative time of sampling from the parameters posterior distribution using HMC with 10 leapfrog steps on sunspot dataset. The GP took 3 s per sample.

Order	GP	SSGP	PSSGP
1	1	4.5	<b>0.55</b>
2	<b>1</b>	5.73	1.36
3	<b>1</b>	6.9	2.55

As we can see in Table 2, while PSSGP is still competitive compared to SSGP for high dimensional SDE representations, its complexity increases with the dimension to the point it eventually does not outperform the standard GP anymore.

## 6 DISCUSSION

We have presented the first sublinear algorithm for learning and inference in Gaussian Processes, leveraging and extending the parallel Kalman filter and smoother equation introduced in Särkkä and Ángel F. García-Fernández [2021]. This allowed us to reduce dramatically the training time for

<sup>2</sup>The data is available at <https://www.esrl.noaa.gov/gmd/ccgg/trends/>

regression problems on large datasets as illustrated by our experiments on synthetic and real datasets.

In addition we found that this method does not scale well in the case when the representation of the Gaussian process involves a stochastic differential equation with high dimensionality, more work is therefore needed in this direction as to further reduce the complexity of parallel state-space GPs. Moreover recent works [Yaghoobi et al., 2021] have suggested that this parallelization technique could also be used for non-linear state-space models, which would then make it possible to extend the presented work to classification and deep state-space Gaussian processes [Zhao et al., 2020].

## Acknowledgements

The authors would like to thank Academy of Finland (projects 321900 and 321891) as well as the doctoral school of Electrical Engineering, Aalto University for funding the research.

## References

- Martín Abadi, Ashish Agarwal, Paul Barham, Eugene Brevdo, Zhifeng Chen, Craig Citro, Greg S. Corrado, Andy Davis, Jeffrey Dean, Matthieu Devin, Sanjay Ghemawat, Ian Goodfellow, Andrew Harp, Geoffrey Irving, Michael Isard, Yangqing Jia, Rafal Jozefowicz, Lukasz Kaiser, Manjunath Kudlur, Josh Levenberg, Dandelion Mané, Rajat Monga, Sherry Moore, Derek Murray, Chris Olah, Mike Schuster, Jonathon Shlens, Benoit Steiner, Ilya Sutskever, Kunal Talwar, Paul Tucker, Vincent Vanhoucke, Vijay Vasudevan, Fernanda Viégas, Oriol Vinyals, Pete Warden, Martin Wattenberg, Martin Wicke, Yuan Yu, and Xiaoqiang Zheng. TensorFlow: Large-scale machine learning on heterogeneous systems, 2015. Software available from tensorflow.org.
- Patrik Axelsson and Fredrik Gustafsson. Discrete-time solutions to the continuous-time differential lyapunov equation with applications to kalman filtering. *IEEE Transactions on Automatic Control*, 60(3):632–643, 2014.
- G. E. Blelloch. Scans as primitive parallel operations. *IEEE Transactions on Computers*, 38(11):1526–1538, 1989.
- G. E. Blelloch. Prefix sums and their applications. Technical Report CMU-CS-90-190, School of Computer Science, Carnegie Mellon University, 1990.
- William L. Brogan. *Modern Control Theory*. Pearson, 3rd edition, 2011.
- Thomas H Cormen, Charles E Leiserson, Ronald L Rivest, and Clifford Stein. *Introduction to Algorithms*. MIT press, 2009.
- Alexander Grigorievskiy, Neil Lawrence, and Simo Särkkä. Parallelizable sparse inverse formulation Gaussian processes (SpInGP). In *IEEE International Workshop on Machine Learning for Signal Processing (MLSP)*, pages 1–6, 2017.
- J. Hartikainen and S. Särkkä. Kalman filtering and smoothing solutions to temporal Gaussian process regression models. In *Proceedings of the IEEE International Workshop on Machine Learning for Signal Processing (MLSP)*, pages 379–384, 2010.
- James Hensman, Nicolas Durrande, and Arno Solin. Variational Fourier features for Gaussian processes. *Journal of Machine Learning Research*, 8(151):1–52, 2017.
- A Scottedward Hodel, Bruce Tenison, and Kameshwar R Poolla. Numerical solution of the Lyapunov equation by approximate power iteration. *Linear Algebra and its Applications*, 236:205–230, 1996.
- N. P. Jouppi, C. Young, N. Patil, D. Patterson, G. Agrawal, R. Bajwa, S. Bates, S. Bhatia, N. Boden, A. Borchers, et al. In-datacenter performance analysis of a tensor processing unit. In *Proceedings of the 44th Annual International Symposium on Computer Architecture*, pages 1–12, 2017.
- Miguel Lázaro-Gredilla, Joaquin Quiñonero-Candela, Carl Edward Rasmussen, and Aníbal R. Figueiras-Vidal. Sparse spectrum Gaussian process regression. *Journal of Machine Learning Research*, 11:1865–1881, 2010.
- Finn Lindgren, Håvard Rue, and Johan Lindström. An explicit link between Gaussian fields and Gaussian Markov random fields: The stochastic partial differential equation approach. *Journal of the Royal Statistical Society: Series B (Statistical Methodology)*, 73(4):423–498, 2011.
- Haitao Liu, Jianfei Cai, Yi Wang, and Yew Soon Ong. Generalized robust Bayesian committee machine for large-scale Gaussian process regression. In *International Conference on Machine Learning*, pages 3131–3140, 2018.
- Kian Hsiang Low, Jiangbo Yu, Jie Chen, and Patrick Jaillet. Parallel Gaussian process regression for big data: Low-rank representation meets Markov approximation. In *Proceedings of the AAAI Conference on Artificial Intelligence*, volume 29, 2015.
- Alexander G. de G. Matthews, Mark van der Wilk, Tom Nickson, Keisuke Fujii, Alexis Boukouvalas, Pablo León-Villagrà, Zoubin Ghahramani, and James Hensman. GPflow: A Gaussian process library using TensorFlow. *Journal of Machine Learning Research*, 18(40):1–6, apr 2017.

- Radford M. Neal. MCMC using Hamiltonian dynamics. In S. Brooks, A. Gelman, G. L. Jones, and X.-L. Meng, editors, *Handbook of Markov Chain Monte Carlo*, chapter 5. Chapman & Hall/CRC, 2011.
- E. E. Osborne. On pre-conditioning of matrices. *Journal of the ACM*, 7(4):338–345, October 1960.
- Joaquin Quiñonero-Candela and Carl Edward Rasmussen. A unifying view of sparse approximate Gaussian process regression. *Journal of Machine Learning Research*, 6: 1939–1959, 2005.
- Carl E. Rasmussen and Christopher K.I. Williams. *Gaussian Processes for Machine Learning*. MIT Press, 2006.
- S. Särkkä, A. Solin, and J. Hartikainen. Spatiotemporal learning via infinite-dimensional Bayesian filtering and smoothing: A look at Gaussian process regression through Kalman filtering. *IEEE Signal Processing Magazine*, 30(4):51–61, 2013. doi: 10.1109/MSP.2013.2246292.
- Simo Särkkä and Ángel F. García-Fernández. Temporal parallelization of Bayesian smoothers. *IEEE Transactions on Automatic Control*, 66(1):299–306, 2021.
- Simo Särkkä and Robert Piché. On convergence and accuracy of state-space approximations of squared exponential covariance functions. In *Proceedings of the IEEE International Workshop on Machine Learning for Signal Processing (MLSP)*, pages 1–6, 2014.
- Simo Särkkä and Arno Solin. *Applied Stochastic Differential Equations*. Cambridge University Press, 2019.
- Simo Särkkä, Arno Solin, and Jouni Hartikainen. Spatiotemporal learning via infinite-dimensional Bayesian filtering and smoothing. *IEEE Signal Processing Magazine*, 30(4):51–61, 2013.
- Arno Solin. *Stochastic Differential Equation Methods for Spatio-Temporal Gaussian Process Regression*. Doctoral dissertation, Aalto University, Helsinki, Finland, 2016.
- Arno Solin and Simo Särkkä. Explicit link between periodic covariance functions and state space models. In *Proceedings of the Seventeenth International Conference on Artificial Intelligence and Statistics (AISTATS)*, volume 33, pages 904–912, 2014.
- Arno Solin and Simo Särkkä. Hilbert space methods for reduced-rank Gaussian process regression. *Statistics and Computing*, 30(2):419–446, 2020.
- Fatemeh Yaghoobi, Adrien Corenflos, Sakira Hassan, and Simo Särkkä. Parallel iterated extended and sigma-point Kalman smoothers. In *To appear in Proceedings of IEEE International Conference on Acoustics, Speech and Signal Processing (ICASSP)*, 2021.
- Michael Minyi Zhang and Sinead A. Williamson. Embarassingly parallel inference for Gaussian processes. *Journal of Machine Learning Research*, 20(169):1–26, 2019.
- Zheng Zhao, Muhammad Emzir, and Simo Särkkä. Deep state-space gaussian processes. *arXiv preprint arXiv:2008.04733*, 2020.